

Analysis of biologically plausible neuron models for regression with spiking neural networks

Mario De Florio
Division of Applied Mathematics
Brown University
Providence, RI
mario_de_florio@brown.edu

Adar Kahana
Division of Applied Mathematics
Brown University
Providence, RI
adar_kahana@brown.edu

George Em Karniadakis
Division of Applied Mathematics
Brown University
Providence, RI
george_karniadakis@brown.edu

Abstract—This paper explores the impact of biologically plausible neuron models on the performance of Spiking Neural Networks (SNNs) for regression tasks. While SNNs are widely recognized for classification tasks, their application to Scientific Machine Learning and regression remains underexplored. We focus on the membrane component of SNNs, comparing four neuron models: Leaky Integrate-and-Fire, FitzHugh–Nagumo, Izhikevich, and Hodgkin-Huxley. We investigate their effect on SNN accuracy and efficiency for function regression tasks, by using Euler and Runge-Kutta 4th-order approximation schemes. We show how more biologically plausible neuron models improve the accuracy of SNNs while reducing the number of spikes in the system. The latter represents an energetic gain on actual neuromorphic chips since it directly reflects the amount of energy required for the computations.

Index Terms—Spiking Neural Networks, LIF model, FitzHugh-Nagumo model, Izhikevich model, Hodgkin-Huxley model, Regression, Scientific Machine Learning

I. INTRODUCTION

The neuromorphic research has been gaining a lot of traction recently. The main reasons are the potential efficiency, that unlocks faster training and inference when using neural networks [1]. Another reason is the scalability. With more neuromorphic hardware [2] and software [3] made available every day, researchers are inclined to explore applying their methods developed on traditional hardware to neuromorphic chips. Finally, the biological plausibility of neuromorphic research is a backwind that drives this research [4]. The core of neuromorphic research is currently Spiking Neural Networks (SNNs). Several works [5]–[9] have shown the superiority of SNNs in terms of efficiency, while also maintaining sufficient accuracy compared to their Artificial Neural Network (ANN) counterparts. Most works so far that utilize SNNs for Machine Learning (ML) focus on classification tasks. This is due to the natural usage of neuromorphic hardware for classification, where the inference is usually binary - 0 if the sample belongs to the specific class and 1 otherwise (also referred to as one-

hot classification). This aligns with the neuronal model well - 0 for no spike and 1 for spike.

A less explored area of neuromorphic research is the use of SNNs for Scientific Machine Learning (SciML). An example of a SciML task would be approximating a continuous function using ML. These problems are often using regression instead of classification, which is a challenge for SNNs since they do not naturally fit the paradigm like in classification. However, to some extent, regression is still possible using SNNs as presented in [10]. Following regression, we have shown that SNNs can be used for operator regression, numerical schemes for dynamical systems [11], physics-informed machine learning [12], and more [13]–[15]. There is still a lot to study, revolving around neuromorphic algorithms for SciML, and this work presents a fundamental step.

SNNs have three main components. The first is the input data, which is in the form of spikes (binary zeros and ones). Data is encoded into spikes before being input into the SNN, and outputs are often decoded back to at the end (depending on the task). The second element is the synapse, which can be thought of as a fully connected layer in the classical deep learning sense. The synapses are trained using learning rules [16]. Last are the membranes, which are analogous to the activation functions. An illustration of the structure of an SNN is presented in Fig. 1 The membranes are the focus of this work.

From the definition of the biological neuron [17], the membrane is a voltage gate at the entrance of the neuronal cell. The membrane “decides” how much voltage enters, and when a certain voltage threshold is crossed the neuron spikes for a short period of time, and the membrane voltage resets to its resting voltage. The first discovery of the membrane model was in 1907 by Louis Lapicque [18], where he injected a frog’s leg with voltage until it twitched, inventing the Leaky-Integrate and Fire (LIF) neuron model that is commonly used in many studies. This model is famous for its simplicity, and also biological accuracy. Many neuroscience studies [19]–[22] use this model, and all SNN software and hardware simulators we are aware of have implementations of a LIF model. The LIF neuron is modeled using a Resistor-Capacitor circuit (hence the term neuron model), as explained in detail in the following section.

This work was supported by the Vannevar Bush Faculty Fellowship award (GEK) from ONR (N00014-22-1-2795). The work of GEK is supported by the U.S. Department of Energy, Advanced Scientific Computing Research program, under the Scalable, Efficient and Accelerated Causal Reasoning Operators, Graphs and Spikes for Earth and Embedded Systems (SEACROGS) project, DE-SC0023191.

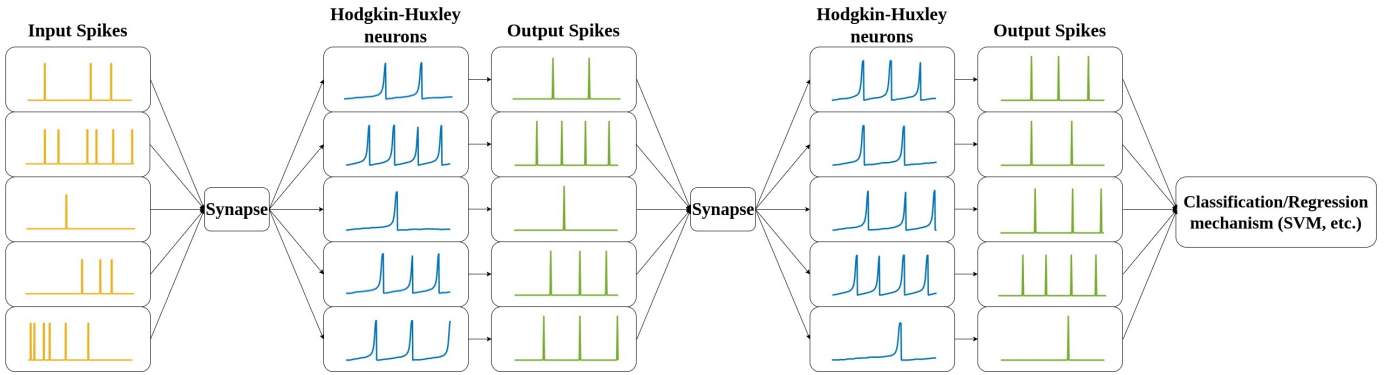


Fig. 1: Sketch of an SNN architecture. The spiking data is used as inputs to Hodgkin-Huxley neurons (membranes) and then fed into a synapse. In this architecture, we have a membrane potential that creates output spikes, followed by a synapse, and another membrane that generates output spikes, followed by a second synapse. Finally, a classification or regression mechanism should be applied. In this study, we employ only one membrane followed by a single synapse to perform regression tasks, as elaborated in the results section.

Several neuroscience-related studies have been conducted to develop more accurate membrane formulations. The FitzHugh-Nagumo model [23], [24] introduces a set of two coupled Ordinary Differential Equations (ODEs) to better capture the oscillatory behavior of the neuronal cell. The Izhikevich model [25] is also a set of ODEs, which captures better the spiking patterns. The Hodgkin-Huxley model [26] is a set of four non-linear coupled ODEs that goes deeper into the transfer of potassium and sodium in and out of the neuronal cell. While the aforementioned three models and LIF are explored in this work, we note that several other models have been proposed [27]–[30]. The trade-off when estimating the eligibility of the models for SciML is between the accuracy of the overall process as described in the Results section and the complexity of the model, which directly impacts its efficiency. These were the guidelines for choosing the models to compare in this work, where LIF is the simplest and most efficient and Hodgkin-Huxley on the other accuracy end of the spectrum. The intermediate ones are, in addition to their qualities, very popular amongst this scientific community.

The main question we explore in this work is: *how do the different membrane models contribute to the success of an SNN?* As mentioned, SNNs are measured by their overall accuracy, as well as their efficiency. We first develop a generic implementation of a SNN with a synapse and a membrane, and simply alternate between the different membrane models. To do this, we implemented all neuron models and fine-tuned the parameters to achieve the desired results. The findings we report in this manuscript bring valuable insights for those experimenting with SNNs. In addition, we find that more complex models, although taking longer to compute, reduce the total number of spikes registered, which means lower overall energy (higher efficiency).

II. BIOLOGICAL NEURON MODELS

A. Leaky Integrate-and-Fire model

The Leaky Integrate-and-Fire (LIF) model is a simplified neuronal model widely used for its computational efficiency and ease of analysis. It provides a basic representation of neuronal dynamics, capturing the essential features of membrane potential integration and action potential generation. The earliest form of the Integrate-and-Fire model was originally introduced by Lapicque in 1907 [18], and subsequently, the LIF model was developed after adding an attenuation term [31].

The dynamics of the LIF model is governed by a single ODE that describes the evolution of the membrane potential $V(t)$ over time:

$$\frac{dV(t)}{dt} = \frac{V(t) - V_{rest}}{RC} + I(t), \quad (1)$$

where C is the membrane capacitance, R is the membrane resistance, $I(t)$ is the input current, and V_{rest} is the membrane resting voltage. In our simulation, $RC = 0.2$ and $I_c(t)$ are input currents of magnitude 1.

The LIF model is commonly used to study the response of a neuron to input currents. A spike is generated when the membrane potential reaches a threshold value $V_{th} = 1$. Upon reaching this threshold, the membrane potential is reset to a resting value V_{rest} . The thresholding mechanism is expressed as follows:

$$\text{if } V \geq V_{th}, \text{ then spike and } V \rightarrow V_{rest} \quad (2)$$

B. FitzHugh–Nagumo model

The FitzHugh–Nagumo (FHN) model is a simplified two-variable system of ODEs that was introduced by Richard FitzHugh in 1961 [23] and later refined by J. Nagumo et al. in 1962 [24]. The FHN model serves as a mathematical ab-

straction to capture the characteristics of neuronal excitability and oscillatory behavior, and it has the following form

$$\begin{cases} \frac{dV}{dt} = V - \frac{V^3}{3} - W + I \\ \frac{dW}{dt} = \frac{1}{\gamma}(V + \alpha - \beta W) \end{cases} \text{ s.t. } \begin{cases} V(0) = 0 \\ W(0) = 0 \end{cases} \quad (3)$$

where V is the membrane potential, W is a recovery variable, and I is the input current. The parameters governing the system's behavior are the bifurcation parameter $\alpha = 0.7$ determining the onset of excitability, $\beta = 0.8$ which controls the recovery variable's sensitivity to the membrane potential, and $\gamma = 12.5$ governs the timescale of the recovery variable. A spike is generated and the membrane resets to the resting value 0 once the threshold value of 1 is reached.

C. Izhikevich model

The Izhikevich model, introduced by Eugene M. Izhikevich in 2003 [25], is a simple yet powerful two-variable neuronal model that captures a wide range of spiking behaviors observed in real neurons. This model is particularly valuable for its computational efficiency and ability to replicate diverse neural firing patterns.

The dynamics of the Izhikevich model are governed by the following set of equations:

$$\begin{cases} \frac{dv}{dt} = 0.04v^2 + 5v + 140 - u + I \\ \frac{du}{dt} = a(bv - u) \end{cases} \text{ s.t. } \begin{cases} v(0) = -70mV \\ u(0) = -14 \end{cases} \quad (4)$$

with the auxiliary condition

$$\text{if } v \geq v_{th}, \text{ then spike and } \begin{cases} v \rightarrow c \\ u \rightarrow u + d \end{cases} \quad (5)$$

where v represents the membrane potential, u is a recovery variable, and $I = 10mA$ is the input current. The parameters shaping the spiking dynamics are $a = 0.02 \frac{1}{ms}$, which controls the time scale of the recovery variable, $b = 0.2$ that influences the sensitivity of the recovery variable to the membrane potential, $c = -50mV$, which is the after-spike reset value of the membrane potential caused by the fast high-threshold K^+ conductances, and $d = 2mV$, which is the after-spike reset of the recovery variable caused by slow high-threshold Na^+ and K^+ conductances.

D. Hodgkin-Huxley model

The Hodgkin-Huxley model, proposed in 1952 by British physiologists Alan Lloyd Hodgkin and Andrew Huxley [26], revolutionized our understanding of the mechanisms underlying the generation and propagation of action potentials in neurons. This mathematical model provides a framework for describing the complex dynamics of ion channels and membrane potentials in excitable cells, particularly neurons. The activation of the membrane potential is described by

the following system of four non-linear Ordinary Differential Equations (ODEs) subject to certain initial conditions [32]:

$$\begin{cases} C_m \frac{dV_m}{dt} = -g_l(V_m - e_l) - g_K n^4(V_m - e_K) \\ \quad - g_{Na} m^3 h(V_m - e_{Na}) + I \\ \frac{dn}{dt} = \alpha_n(V_m)(1 - n) - \beta_n(V_m)n \\ \frac{dm}{dt} = \alpha_m(V_m)(1 - m) - \beta_m(V_m)m \\ \frac{dh}{dt} = \alpha_h(V_m)(1 - h) - \beta_h(V_m)h \end{cases} \quad (6)$$

subject to $V_m(0) = -65mV$, $n(0) = 0.3177$, $m(0) = 0.0529$, and $h(0) = 0.5960$. Each ODE describes the time evolution of the four variables of the HH model. In particular, V_m is the membrane potential, n and m are the activation gating variables for potassium and sodium channels, respectively, and h is the inactivation gating variable for the sodium channels. C_m represents the membrane capacitance, g_l , g_K and g_{Na} are the leak, potassium and sodium conductances, respectively, e_l , e_K and e_{Na} are their reversal potentials, and I is the input current per unit area. The α and β functions represent the rate constants for the ion channels, and they can be expressed as

$$\begin{aligned} \alpha_n(V_m) &= \frac{0.1 - 0.01U_{m0}}{e^{1-0.1U_{m0}} - 1} & \beta_n(V_m) &= 0.125e^{-\frac{U_{m0}}{80}} \\ \alpha_m(V_m) &= \frac{2.5 - 0.1U_{m0}}{e^{2.5-0.1U_{m0}} - 1} & \beta_m(V_m) &= 4e^{-\frac{U_{m0}}{18}} \\ \alpha_h(V_m) &= 0.07e^{-\frac{U_{m0}}{20}} & \beta_h(V_m) &= \frac{1}{1 + e^{-\frac{U_{m0}}{10}}} \end{aligned}$$

where $U_{m0} = V_m - V_m(0)$, with $V_m(0) = -65mV$, and the values of the parameters used in our simulations, assuming $1cm^2$ of membrane, are $C_m = 1\mu F$, $g_l = 0.3mS$, $g_K = 36mS$, $g_{Na} = 120mS$, $e_K = -77mV$, $e_l = -54mV$, $e_{Na} = 50mV$. In our simulations, the input current I is represented by spikes of $5mA$ of intensity. The membrane has a threshold parameter set at $30mV$. When the membrane potential reaches the threshold, a spike is registered in the neuron, and the membrane resets to the value of $V_m(0)$. An example of this membrane's behavior is represented in Figure 2.

III. NUMERICAL METHODS

A. Euler method

To simplify the calculations, we can employ the forward Euler finite difference method to directly approximate the solution of the Hodgkin-Huxley model [33] from equations (6), as follows:

$$\begin{aligned} V_m(t + \Delta t) &= V_m(t) + \Delta t(I(t) - g_K n^4(V_m(t) - e_K) \\ &\quad - g_{Na} m^3 h(V_m(t) - e_{Na}) - g_L(V_m(t) - e_L))/C_m \\ n(t + \Delta t) &= n(t) + \Delta t(\alpha_n(1 - n(t)) - \beta_n n(t)) \\ m(t + \Delta t) &= m(t) + \Delta t(\alpha_m(1 - m(t)) - \beta_m m(t)) \\ h(t + \Delta t) &= h(t) + \Delta t(\alpha_h(1 - h(t)) - \beta_h h(t)) \end{aligned} \quad (7)$$

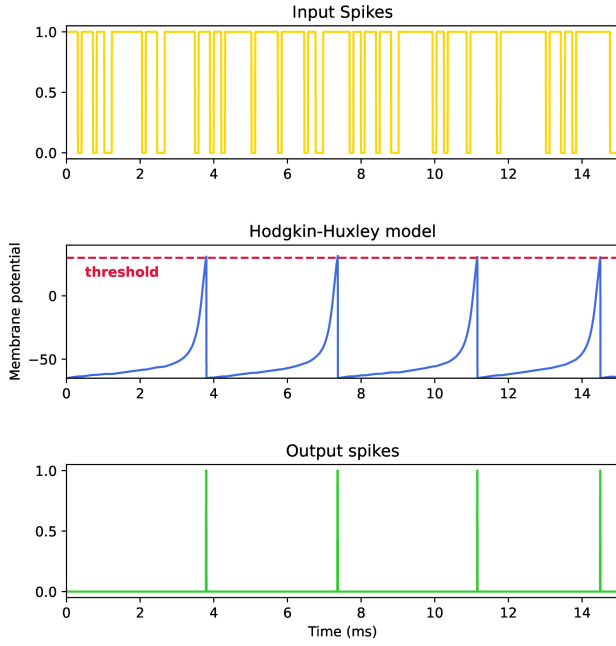


Fig. 2: Example of the membrane potential over time for given input spikes. The reset mechanism is set to a resting position without refraction. The top plot presents the input spikes over time. The middle plot presents the membrane activity modeled by the Hodgkin-Huxley model. Notice that when the membrane potential reaches the threshold, an output spike is registered, and the membrane resets. The bottom plot presents the registered output spikes over time.

where Δt is set equal to 0.1. This serves as a simplified approximation to the solution of the Hodgkin-Huxley model, and it's anticipated that the accuracy in computing the membrane potential will be reduced. Nevertheless, this approach offers a more lightweight implementation, enabling more efficient computations.

B. Runge-Kutta 4th order method

In contrast to the Euler method, the Runge-Kutta 4th Order (RK4) numerical integration scheme provides a more accurate approximation of the solution to the Hodgkin-Huxley model [34]. The RK4 method involves multiple steps to iteratively update the variables, providing enhanced accuracy in capturing the intricate dynamics of the membrane potential and gating variables.

The slopes k_1, k_2, k_3 , and k_4 for all the HH variables are

$$\begin{aligned}
 k_{1V} &= \Delta t (I - g_K n^4 (V_m - e_K) - g_{Na} m^3 h (V_m - e_{Na}) \\
 &\quad - g_L (V_m - e_L)) / C_m \\
 k_{1n} &= \Delta t (\alpha_n (1 - n) - \beta_n n) \\
 k_{1m} &= \Delta t (\alpha_m (1 - m) - \beta_m m) \\
 k_{1h} &= \Delta t (\alpha_h (1 - h) - \beta_h h)
 \end{aligned} \tag{8}$$

$$\begin{aligned}
 k_{2V} &= \Delta t (I - g_K (n + 0.5k_{1n})^4 (V_m + 0.5k_{1V} - e_K) \\
 &\quad - g_{Na} (m + 0.5k_{1m})^3 (h + 0.5k_{1h}) (V_m + 0.5k_{1V} - e_{Na}) \\
 &\quad - g_L (V_m + 0.5k_{1V} - e_L)) / C_m \\
 k_{2n} &= \Delta t (\alpha_n (1 - (n + 0.5k_{1n})) - \beta_n (n + 0.5k_{1n})) \\
 k_{2m} &= \Delta t (\alpha_m (1 - (m + 0.5k_{1m})) - \beta_m (m + 0.5k_{1m})) \\
 k_{2h} &= \Delta t (\alpha_h (1 - (h + 0.5k_{1h})) - \beta_h (h + 0.5k_{1h}))
 \end{aligned} \tag{9}$$

$$\begin{aligned}
 k_{3V} &= \Delta t (I - g_K (n + 0.5k_{2n})^4 (V_m + 0.5k_{2V} - e_K) \\
 &\quad - g_{Na} (m + 0.5k_{2m})^3 (h + 0.5k_{2h}) (V_m + 0.5k_{2V} - e_{Na}) \\
 &\quad - g_L (V_m + 0.5k_{2V} - e_L)) / C_m \\
 k_{3n} &= \Delta t (\alpha_n (1 - (n + 0.5k_{2n})) - \beta_n (n + 0.5k_{2n})) \\
 k_{3m} &= \Delta t (\alpha_m (1 - (m + 0.5k_{2m})) - \beta_m (m + 0.5k_{2m})) \\
 k_{3h} &= \Delta t (\alpha_h (1 - (h + 0.5k_{2h})) - \beta_h (h + 0.5k_{2h}))
 \end{aligned} \tag{10}$$

$$\begin{aligned}
 k_{4V} &= \Delta t (I - g_K (n + k_{3n})^4 (V_m + k_{3V} - e_K) \\
 &\quad - g_{Na} (m + k_{3m})^3 (h + k_{3h}) (V_m + k_{3V} - e_{Na}) \\
 &\quad - g_L (V_m + k_{3V} - e_L)) / C_m \\
 k_{4n} &= \Delta t (\alpha_n (1 - (n + k_{3n})) - \beta_n (n + k_{3n})) \\
 k_{4m} &= \Delta t (\alpha_m (1 - (m + k_{3m})) - \beta_m (m + k_{3m})) \\
 k_{4h} &= \Delta t (\alpha_h (1 - (h + k_{3h})) - \beta_h (h + k_{3h}))
 \end{aligned} \tag{11}$$

Thus, the updated equations for the RK4 method applied to the Hodgkin-Huxley model are as follows:

$$\begin{aligned}
 V_m(t + \Delta t) &= V_m + \frac{1}{6} (k_{1V} + 2k_{2V} + 2k_{3V} + k_{4V}) \\
 n(t + \Delta t) &= n + \frac{1}{6} (k_{1n} + 2k_{2n} + 2k_{3n} + k_{4n}) \\
 m(t + \Delta t) &= m + \frac{1}{6} (k_{1m} + 2k_{2m} + 2k_{3m} + k_{4m}) \\
 h(t + \Delta t) &= h + \frac{1}{6} (k_{1h} + 2k_{2h} + 2k_{3h} + k_{4h})
 \end{aligned} \tag{12}$$

Here, Δt is the time step, and V_m, n, m , and h represent the membrane potential and gating variables. The RK4 method ensures a more accurate numerical approximation of the Hodgkin-Huxley model's dynamics compared to the Euler method, making it suitable for simulations that require higher precision.

IV. RESULTS AND DISCUSSIONS

To test the performance of the different neural models computed with the Euler and RK4 methods we follow the experimental setup presented in [10] for function regression. We use the same codes, changing only the activation from LIF neurons into the various ones presented in this work. Since we do not have access to a neuromorphic chip for testing the method with spikes, we are using a GPU-based training with TensorFlow 2 [35]. The energetic gains are measured by the number of spikes in the system, rather than execution time. This is a valid measure, as on an actual chip the number of

spikes directly reflects the amount of energy required for the computations.

The SNN architecture we use is a membrane layer, followed by a synapse. Since we are not using a neuromorphic chip, we use the back-propagation algorithm to train the synapse and learn the weights of the network. The shallow network we choose here is sufficient for demonstrating the advantages of using different membrane models and analyzing the results. We point out that using a more complex network architecture will likely yield better performance. In addition, with this specific architecture, the back-propagation algorithm operates only on the last layer, which is considered more “biologically plausible”. The input data are encoded using $N_t = 150$ time steps and $N_x = 100$ collocation points for spatial discretization. The outputs are floating numbers (no decoding required). The three functions we attempt for regression, with and without noise, are:

- *Square*

$$y(x) = x^2 \quad (13)$$

- *Discontinuity*

$$y(x) = \begin{cases} 1 & \text{for } x \leq 0 \\ 2 & \text{for } x > 0 \end{cases} \quad (14)$$

- *Sine*

$$y(x) = \frac{\sin(kx)}{k^2} \quad \text{with } k = 1.2 \quad (15)$$

The square function is more of a sanity check. The discontinuous function is challenging, since it has a sharp jump (not differentiable), and the sine oscillates around 0 which often causes issues. We also consider the cases in which the functions are perturbed with 0.1 additive normally distributed noise. The performance of the regression is reported in terms of the L_2 -norm difference between the predicted and exact solution as

$$L_2\text{-norm} = \sum_{j=1}^{N_x} (y_{pred}(x_j) - y_{exact}(x_j))^2, \quad (16)$$

where N_x is the number of collocation points of the spatial discretization. In Figure 3, a qualitative visualization of the regressions made by using the Euler method for the LIF and HH models is reported for the three functions, with and without noise. One can see how with HH there is a better overlap with the exact solutions. To quantitatively evaluate the different performances in terms of the L_2 -norm, efficiency (number of spikes produced), and computational times we can refer to Table I. As expected, the computational time increases from Euler to RK4, and from 1-ODE model (LIF) to 4-ODE model (HH), with a decrease in the L_2 -norm error. One can see that in terms of accuracy, IZH and HH outperform LIF and FHN neuron models for all the test cases, but with a significant cost in computational time. It is interesting to notice how a greater accuracy corresponds to a lower number of output spikes, which results in a more efficient cost for the neuromorphic hardware in regression tasks.

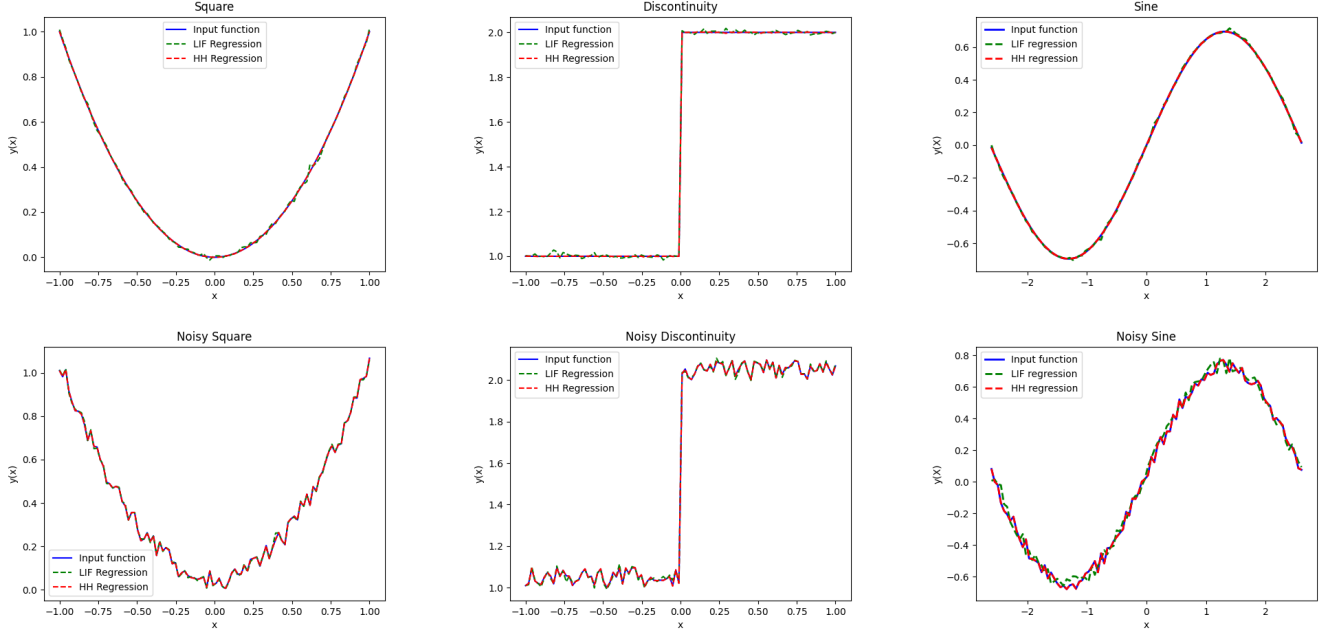


Fig. 3: Comparison of function regressions using LIF model and Hodgkin-Huxley model with Euler method in the SNN implementation for three different functions, with and without noise.

TABLE I: Relative L_2 error and number of output spikes for neuron membrane models and solvers, for both noiseless and noisy functions. The encoded neuron models are Leaky Integrate-and-Fire (LIF), FitzHugh–Nagumo (FHN), Izhikevich (IZH), and Hodgkin-Huxley (HH).

Neuron model	Numerical method	Relative L_2 error (# of output spikes)						Time (s)
		Noiseless			Noisy			
		Discontinuity	Square	Sine	Discontinuity	Square	Sine	
LIF	Euler	4.50e-03 (2271)	1.30e-02 (2242)	1.43e-02 (2312)	4.30e-03 (2257)	1.18e-02 (2212)	1.52e-02 (2225)	12
	RK	1.864e-03 (904)	6.13e-03 (886)	5.82e-03 (896)	1.66e-03 (908)	4.78e-03 (902)	5.53e-03 (897)	22
FHN	Euler	6.63e-04 (281)	1.96e-03 (269)	1.87e-03 (271)	5.84e-04 (266)	2.03e-03 (276)	2.19e-03 (272)	16
	RK	6.16e-04 (55)	5.49e-04 (53)	6.10e-04 (51)	6.24e-04 (58)	5.02e-04 (54)	6.40e-04 (56)	48
IZH	Euler	5.78e-04 (219)	2.20e-03 (222)	2.05e-03 (217)	6.58e-04 (216)	1.97e-03 (218)	1.91e-03 (221)	20
	RK	5.16e-04 (58)	5.67e-04 (62)	5.89e-04 (64)	5.52e-04 (65)	6.11e-04 (67)	7.32e-04 (66)	55
HH	Euler	4.17e-04 (118)	1.26e-03 (114)	1.24e-03 (122)	4.61e-04 (113)	1.20e-03 (109)	1.37e-03 (121)	48
	RK	1.69e-03 (71)	1.02e-03 (71)	8.95e-04 (62)	9.20e-04 (74)	8.07e-04 (74)	9.04e-04 (86)	130

REFERENCES

- [1] D. Marković, A. Mizrahi, D. Querlioz, and J. Grollier, “Physics for neuromorphic computing,” *Nature Reviews Physics*, vol. 2, no. 9, pp. 499–510, 2020, Nature Publishing Group UK London.
- [2] J. Schemmel, D. Brüderle, A. Grübl, M. Hock, K. Meier, and S. Millner, “A wafer-scale neuromorphic hardware system for large-scale neural modeling,” in *2010 IEEE International Symposium on Circuits and Systems (ISCAS)*, pp. 1947–1950, 2010, IEEE.
- [3] T. Titirsha, S. Song, A. Balaji, and A. Das, “On the role of system software in energy management of neuromorphic computing,” in *Proceedings of the 18th ACM International Conference on Computing Frontiers*, pp. 124–132, 2021.
- [4] J.-Q. Yang, R. Wang, Y. Ren, J.-Y. Mao, Z.-P. Wang, Y. Zhou, and S.-T. Han, “Neuromorphic engineering: from biological to spike-based hardware nervous systems,” *Advanced Materials*, vol. 32, no. 52, p. 2003610, 2020, Wiley Online Library.
- [5] B. Han and K. Roy, “Deep spiking neural network: Energy efficiency through time based coding,” in *European Conference on Computer Vision*, pp. 388–404, 2020, Springer.
- [6] S. Misra, C. Allemang, C. Arose, B. Taylor, A. Dubovskiy, A. Sidi El Valli, L. Rehm, A. Haas, A. Kent, L. Bland, S. Cardwell, D. Smith and J.B. Aimone, *How to use stochastic devices in probabilistic calculations*, Bulletin of the American Physical Society, 2024.
- [7] E. Lemaire, L. Cordone, A. Castagnetti, P.-E. Novac, J. Courtois, and B. Miramond, “An analytical estimation of spiking neural networks energy efficiency,” in *International Conference on Neural Information Processing*, pp. 574–587, 2022, Springer.
- [8] R. V. W. Putra and M. Shafique, “Fspinn: An optimization framework for memory-efficient and energy-efficient spiking neural networks,” *IEEE Transactions on Computer-Aided Design of Integrated Circuits and Systems*, vol. 39, no. 11, pp. 3601–3613, 2020, IEEE.
- [9] S. Park, S. Kim, H. Choe, and S. Yoon, “Fast and efficient information transmission with burst spikes in deep spiking neural networks,” in *Proceedings of the 56th Annual Design Automation Conference 2019*, pp. 1–6, 2019.
- [10] A. Kahana, Q. Zhang, L. Gleyzer, and G. E. Karniadakis, “Function regression using spiking deepnet,” *arXiv preprint arXiv:2205.10130*, 2022.
- [11] S. O. Fatunla, *Numerical methods for initial value problems in ordinary differential equations*, Academic Press, 2014.
- [12] G. E. Karniadakis, I. G. Kevrekidis, L. Lu, P. Perdikaris, S. Wang, and L. Yang, “Physics-informed machine learning,” *Nature Reviews Physics*, vol. 3, no. 6, pp. 422–440, 2021, Nature Publishing Group UK London.
- [13] Q. Yu, H. Tang, K. C. Tan, and H. Yu, “A brain-inspired spiking neural network model with temporal encoding and learning,” *Neurocomputing*, vol. 138, pp. 3–13, 2014, Elsevier.
- [14] H. Mostafa, “Supervised learning based on temporal coding in spiking neural networks,” *IEEE Transactions on Neural Networks and Learning Systems*, vol. 29, no. 7, pp. 3227–3235, 2017, IEEE.
- [15] I. M. Comsa, K. Potempa, L. Versari, T. Fischbacher, A. Gesmundo, and J. Alakuijala, “Temporal coding in spiking neural networks with alpha synaptic function,” in *ICASSP 2020-2020 IEEE International Conference on Acoustics, Speech and Signal Processing (ICASSP)*, pp. 8529–8533, 2020, IEEE.
- [16] Y. Bengio, S. Bengio, and J. Cloutier, *Learning a synaptic learning rule*, Citeseer, 1990.
- [17] I. B. Levitan and L. K. Kaczmarek, *The neuron: Cell and molecular biology*, Oxford University Press, USA, 2015.
- [18] L. M. Lapicque, “Recherches quantitatives sur l’excitation électrique des nerfs,” *J Physiol Paris*, vol. 9, pp. 620–635, 1907.
- [19] C. Laing and G. J. Lord, *Stochastic methods in neuroscience*, Oxford University Press, 2009.
- [20] S. Ostojic and N. Brunel, “From spiking neuron models to linear-nonlinear models,” *PLoS computational biology*, vol. 7, no. 1, p. e1001056, 2011, Public Library of Science San Francisco, USA.
- [21] S. Krasovskaya and W. J. MacInnes, “Saliency models: A computational cognitive neuroscience review,” *Vision*, vol. 3, no. 4, p. 56, 2019, MDPI.
- [22] R. E. Kass, S.-I. Amari, K. Arai, E. N. Brown, C. O. Diekmann, M. Diesmann, B. Doiron, U. T. Eden, A. L. Fairhall, G. M. Fiddymant, and others, “Computational neuroscience: Mathematical and statistical perspectives,” *Annual review of statistics and its application*, vol. 5, pp. 183–214, 2018, Annual Reviews.
- [23] R. FitzHugh, “Impulses and physiological states in theoretical models of nerve membrane,” *Biophysical journal*, vol. 1, no. 6, pp. 445–466, 1961, Elsevier.
- [24] J. Nagumo, S. Arimoto, and S. Yoshizawa, “An active pulse transmission line simulating nerve axon,” *Proceedings of the IRE*, vol. 50, no. 10, pp. 2061–2070, 1962, IEEE.
- [25] E. M. Izhikevich, “Simple model of spiking neurons,” *IEEE Transactions on neural networks*, vol. 14, no. 6, pp. 1569–1572, 2003, IEEE.
- [26] A. L. Hodgkin and A. F. Huxley, “A quantitative description of membrane current and its application to conduction and excitation in nerve,” *The Journal of physiology*, vol. 117, no. 4, p. 500, 1952, Wiley-Blackwell.
- [27] P. F. Pinsky and J. Rinzel, “Intrinsic and network rhythmogenesis in a reduced Traub model for CA3 neurons,” *Journal of computational neuroscience*, vol. 1, pp. 39–60, 1994, Springer.
- [28] S. Hayman, “The McCulloch-Pitts Model,” in *IJCNN’99. International Joint Conference on Neural Networks. Proceedings (Cat. No. 99CH36339)*, vol. 6, pp. 4438–4439, 1999, IEEE.
- [29] H. Lecar, “Morris-Lecar model,” *Scholarpedia*, vol. 2, no. 10, p. 1333, 2007.
- [30] M. Storace, D. Linaro, and E. de Lange, “The Hindmarsh–Rose neuron model: Bifurcation analysis and piecewise-linear approximations,” *Chaos: An Interdisciplinary Journal of Nonlinear Science*, vol. 18, no. 3, 2008, AIP Publishing.
- [31] L. F. Abbott, “Lapicque’s introduction of the integrate-and-fire model neuron (1907),” *Brain research bulletin*, vol. 50, no. 5-6, pp. 303–304, 1999, Citeseer.
- [32] W. Teka, D. Stockton, and F. Santamaria, “Power-law dynamics of membrane conductances increase spiking diversity in a Hodgkin-Huxley model,” *PLoS computational biology*, vol. 12, no. 3, p. e1004776, 2016, Public Library of Science San Francisco, CA USA.
- [33] M. Hanslien, K. H. Karlsen, and A. Tveito, “A maximum principle for an explicit finite difference scheme approximating the Hodgkin-Huxley model,” *BIT Numerical Mathematics*, vol. 45, pp. 725–741, 2005, Springer.
- [34] J. W. Moore and F. Ramon, “On numerical integration of the Hodgkin and Huxley equations for a membrane action potential,” *Journal of theoretical Biology*, vol. 45, no. 1, pp. 249–273, 1974, Elsevier.
- [35] S. Raschka and V. Mirjalili, *Python machine learning: Machine learning and deep learning with Python, scikit-learn, and TensorFlow 2*, Packt Publishing Ltd, 2019.